THE IDENTIFICATION OF A ROTOR BEND FROM VIBRATION MEASUREMENTS

S. Edwards[1], A.W. Lees[2] and M.I. Friswell[3]

University of Wales, Swansea
Department of Mechanical Engineering
Singleton Park
Swansea SA2 8PP, UK

ABSTRACT. Unbalance and bends in rotating shafts both give rise to force excitation at a frequency corresponding to once per revolution. Because of detailed differences in the variation of the forcing with speed, it is possible to distinguish between these two phenomena by observing the machine's behaviour over a range of speeds, normally during the run down from normal operating speed to rest. In this paper, a method is presented to determine the modal components of a bend, and hence the bend geometry, from measured vibration signals. The only requirement is a good numerical model of the rotor. No information is required concerning the supporting structure, although if only vibration data at the pedestals is available, an approximate bearing model is needed. However, if shaft motion is also measured, no information about the bearings is required. The calculation is presented in two directions orthogonal to the rotor, and it is shown how the method can determine the extent and location of a bend in the presence of noisy data and unbalance.

NOMENCLATURE

x	axial distance along rotor
y	displacement orthogonal to rotor
z	second orthogonal direction
L	rotor length
G	rotor Green's function
F	force on rotor
β	bend modal coefficients
c	number of bend modes
e	unbalance
d	number of unbalance planes
n	number of bearings
m	bend mode number
k	bearing stiffness
$[a]$	force sensitivity matrix at a given frequency
G_{ij}	discrete representation of G
EI	rotor bending stiffness
$[K_s]$	rotor stiffness matrix
$[K]$	foundation stiffness matrix
$[M]$	foundation mass matrix
$[w]$	frequency dependent matrix of displacements
$\{v\}$	vector of unknown components
$[W]$	concatenation of $[w]$
$[q]$	bend influence matrix defined in (13)
$[Q]$	concatenation of $[q]$
$[u]$	unbalance influence matrix
$[U]$	concatenation of $[u]$
$[p]$	force influence matrix
$\{P\}$	generalised force vector defined in (17)
δ	Kronecker delta
ω	angular frequency
ω_m	natural frequency
ρ	rotor mass per unit length
ψ, Ψ	rotor free-free modes

[1] PhD Student, Simon.Edwards@swansea.ac.uk
[2] Professor, A.W.Lees@swansea.ac.uk
[3] Senior Lecturer, M.I.Friswell@swansea.ac.uk

Subscripts

i,j	counters
bi	bearing *i*
m	bend mode
r	rotor
p	pedestal

1. INTRODUCTION

Increased running speeds and the requirement for rotating machinery to operate within specified levels of vibration mean that the strict control of machinery vibration is essential in today's industry. Of the many different causes of rotor vibration, mass unbalance and bent shafts are amongst the most frequently occurring. The phenomenon of shaft forcing due to an initial bend has had an increased amount of research invested in it over the last twenty years or so, albeit much less than mass unbalance. Bends in shafts may be caused in several ways: creep, thermal distortion, previous large unbalance force. The forcing caused by the bend is similar, though slightly different, to that caused by conventional mass unbalance. Shaft bow response causes different amplitude and phase angle relationships than is found with ordinary mass unbalance, which is a function of the square of the speed. It is important to be able to diagnose shaft bow from vibration measurements and thus distinguish between it and mass unbalance.

One of the first extensive investigations into shaft bow was made by Nicholas *et al.* [1,2], in a series of two papers. Part I (Unbalance Response) [1] discusses the unbalance response of flexible rotors due to shaft bow. Part II (Balancing) [2] proposes the balancing theory and gives experimental results for the balancing of a flexible rotor with shaft bow. A broad range of numerical tests were performed to compare responses by looking at amplitude and phase angle behaviour under various conditions. One important conclusion drawn from these tests is that the change in phase angle from rest, up to the speed where maximum rotor amplitude occurs, is not usually 90°, as it is with conventional unbalance. Also, when the bow is 180° out of phase with the unbalance, there always exists a speed (equal to the square root of the residual bow) at which the rotor amplitude is zero. Parkinson *et al.* [3] described the differences in whirl experienced by a rotating shaft subject to shaft bow and mass unbalance. By balancing the net whirl (total whirl minus shaft bow), which contains certain components due to mass unbalance and others due to shaft bow, the residual total whirl at running speed is approximately equal to the shaft bow. For practical applications this is more desirable than simply balancing the total whirl, which leaves a residual bow at non-critical speeds and is only balanced at resonance. The reader is also referred to the treatment of bent shaft behaviour investigated by Meacham *et al.* [4], Flack *et al.* [5] and Salamone and Gunter [6,7].

There have been numerous cases in industry where vibration has been assumed to have arisen from mass unbalance and rotors have been balanced using traditional balancing procedures. This has repeatedly left engineers puzzled as to why vibration persists after balancing and vibration levels may indeed even be worse than before balancing took place. It is therefore important to be able to easily identify a bend and thus make the distinction between it and the more common mass unbalance. This paper extends the unbalance identification method developed by Lees and Friswell [8] to include the identification of a bend. With an accurate rotor model and a certain amount of information concerning bearing characteristics, it is shown how a bent rotor may be identified from vibration measurements at the bearing pedestals. The method is also developed to include the identification of a rotor-bearing system containing both a bend and an unbalance.

2. SYSTEM FORCES

In the following analysis, the shaft bend geometry shall be expressed in terms of the free-free modal properties of the rotor, which can be readily determined, given a model of the shaft. Since dominant damping effects are usually due to bearings, no rotor or support damping is included. The bend profile may be described as

$$y_{bend}(x) = \sum_{m=1}^{\infty} \beta_m \psi_m(x) \tag{1}$$

where ψ_m are the free-free mass normalised rotor modes and β_m the corresponding modal coefficients. The resulting force per unit length due to the bend is then

$$F_{bend}(x) = \frac{\partial^2}{\partial x^2}\left(EI(x) \frac{\partial^2 y_{bend}(x)}{\partial x^2} \right) \tag{2}$$

At an arbitrary position on the shaft, *x*, the displacement is given by

$$y_r(x) = \int_0^L G(\omega, x, x') F(x') dx' \tag{3}$$

where *F(x')* is the force per unit length acting on the rotor and *G(ω,x,x')* is the rotor Green's function, giving the response at position *x* due to a unit force applied at position *x'* [8].

The rotor experiences two kinds of forcing: the unknown bearing reactions $F_{b1},...,F_{bn}$ at *n* bearing stations $x_{b1},...,x_{bn}$ and the force due to the bent shaft profile described above. The total forcing acting on the rotor is then

$$F(x,\omega) = \sum_{m=1}^{\infty} \beta_m \frac{d^2}{dx^2}\left(EI(x) \frac{d^2 \psi_m(x)}{dx^2} \right) + \sum_{i=1}^{n} F_{bi}\, \delta(x - x_{bi}) \tag{4}$$

where δ is the Dirac delta function. Combining equations (3) and (4) then yields an equation for the displacement of the shaft at any position *x* along its length. Writing this displacement equation using the notation

$[G_{bend}]_{mm} = \dfrac{1}{\omega^2 - \omega_m{}^2}$ and $\hat{k}_m = \omega_m{}^2$, where

$\omega_m{}^2 = \int_0^L \psi_m(x) \dfrac{d^2}{dx^2}\left(EI(x) \dfrac{d^2\psi_m(x)}{dx^2} \right) dx$ gives

$$y_r(x) = \sum_{m=1}^{\infty} [G_{bend}]_{mm} \hat{k}_m \beta_m \psi_m(x) + \sum_{i=1}^{n} G(\omega, x, x_{bi}) F_{bi} \qquad (5)$$

Using the result given in [8] for the bearing reaction forces

$$F_{bi} = -k_i (y_{ri} - y_{pi}) \qquad (6)$$

where k_i is the stiffness of bearing i and n (or $2n$ for two directions) measured values of pedestal displacement y_{pi} then a set of simultaneous equations are obtained, which describe the rotor displacement at the bearing locations. It was shown [8] how speed-dependent damping could be included in the analysis, although for the purpose of clarity it has been omitted. Shaft displacement is then

$$y_{rj} = \sum_{m=1}^{\infty} [G_{bend}]_{mm} \hat{k}_m \beta_m \psi_m(x_{bj}) + \sum_{i=1}^{n} k_i (y_{ri} - y_{pi}) G(\omega, x_{bj}, x_{bi}) \qquad (7)$$

Hence, given the shaft profile and pedestal displacements y_{pi} then the reaction forces at the bearings may be determined. Multiplying (5) by k_j

$$k_j y_{rj} = k_j \sum_{m=1}^{\infty} [G_{bend}]_{mm} \hat{k}_m \beta_m \psi_m(x_{bj}) + k_j \sum_{i=1}^{n} G(\omega, x_{bj}, x_{bi}) F_{bi} \qquad (8)$$

and combining equations (6) and (8) leads to the following result for each plane of vibration at each bearing

$$-F_{bj} + k_j y_{pj} = k_j \sum_{m=1}^{\infty} [G_{bend}]_{mm} \hat{k}_m \beta_m \psi_m(x_{bj}) + \sum_{i=1}^{n} G(\omega, x_{bj}, x_{bi}) F_{bi} \qquad (9)$$

Using the notation $G_{pq} = G(\omega, x_{bp}, x_{bq})$ equation (9) can thus be expressed as

$$\begin{Bmatrix} F_1 \\ . \\ . \\ . \\ F_n \end{Bmatrix} = [a]^{-1} \begin{Bmatrix} k_1 y_{p1} - k_1 \sum_{m=1}^{\infty} [G_{bend}]_{mm} \hat{k}_m \beta_m \psi_m(x_{bj}) \\ . \\ . \\ . \\ k_n y_{pn} - k_n \sum_{m=1}^{\infty} [G_{bend}]_{mm} \hat{k}_m \beta_m \psi_m(x_{bj}) \end{Bmatrix} \qquad (10)$$

where

$$a_{ij} = \delta_{ij} + k_i G_{ij} \qquad (11)$$

δ_{ij} is the Kronecker delta and i and j apply over the complete set of bearings. It can be seen from equation (10) that the bearing forces are proportional to the bearing stiffnesses but are independent of foundation stiffness, and although the effects of foundation stiffness will obviously have a large effect on the measured response values, this is dealt with by the fact that the response is indeed measured. This method and the conditioning of the matrix [a] are discussed in detail by Lees and Friswell [9] and Friswell *et al.* [10].

3. IDENTIFICATION METHOD

In order to successfully identify the bend geometry it is necessary to be able to identify the modal coefficients β in equation (1), the free-free modes being known. This unknown vector may be written $\{\beta\} = \{\beta_1, \ldots, \beta_c\}^T$, where c is the maximum number of modes being considered. Adopting this notation allows equation (10) to be written in vector form as

$$\{F\} = [a]^{-1}[k_B]\{y_p\} - [a]^{-1}[k_B][G_{bend}][K_S][\Psi]\{\beta\} \qquad (12)$$

where $[k_B] = \text{diag}(k_1, k_2, \ldots, k_n)$, $\{y_p\} = \{y_{p1}, y_{p2}, \ldots, y_{pn}\}^T$,

$[G_{bend}] = diag\left[\dfrac{1}{\omega^2 - \omega_m{}^2}\right]$, $[K_S] = diag[\hat{k}_m]$ and $[\Psi]$ contains the shaft free-free modes. Substituting $[p] = [a]^{-1}[k_B]$ and $[q] = [a]^{-1}[k_B][G_{bend}][K_S][\Psi]$ gives

$$\{F\} = [p]\{y_p\} - [q]\{\beta\} \qquad (13)$$

$\{F\}$ is the reaction of the bearings on the rotor, its dimension being the number of bearings in the system (x2 for both perpendicular directions). The force due to the bearings acting on the supports is $-\{F\}$.

The unknown foundation forces may be expressed in terms of the foundation mass and stiffness matrices [K] and [M], which are assumed to be symmetric. No damping from the foundations is included since it is found in practice to be negligible in comparison to the damping produced by the bearings. The force acting on the bearings due to the foundations at each measured frequency is

$$-\{F\} = [K]\{y_p\} - \omega^2[M]\{y_p\} \qquad (14)$$

These unknown matrices in equation (13) are now re-arranged in the form

$$-\{F\} = [w(\omega)]\{v\} \qquad (15)$$

where [w] is the matrix containing the terms relating to $\{y_p\}$, taking the form

$$[w(\omega)] = \begin{bmatrix} y_{p1}(\omega) & 0 \\ 0 & y_{p2}(\omega) \\ y_{p2}(\omega) & y_{p1}(\omega) \\ -\omega^2 y_{p1}(\omega) & 0 \\ 0 & -\omega^2 y_{p2}(\omega) \\ -\omega^2 y_{p2}(\omega) & -\omega^2 y_{p1}(\omega) \end{bmatrix}^T$$

for the two degrees of freedom case. $\{v\}$ contains the relevant terms of $[K]$ and $[M]$ and has been designated the order $\{v\} = \{k_{11} \quad k_{22} \quad k_{12} \quad m_{11} \quad m_{22} \quad m_{12}\}^T$, where k_{ij} and m_{ij} are the (i,j)th elements of $[K]$ and $[M]$ respectively.

Equating (13) and (15) at each frequency step

$$-[w(\omega)]\{v\} = [p]\{y_p\} - [q(\omega)]\{\beta\} \tag{16}$$

and including each step over the whole frequency range gives

$$[W]\{v\} + [Q]\{\beta\} = \{P\} \tag{17}$$

where $[W]$, $[Q]$ and $\{P\}$ are simply the concatenation of each sub-matrix through the considered range. Re-writing equation (17) as

$$[W\,Q]\begin{Bmatrix} v \\ \beta \end{Bmatrix} = \{P\} \tag{18}$$

allows like terms to be grouped and, using the Moore-Penrose pseudo-inverse for the over-determined problem, the following least squares solution is obtained

$$\begin{Bmatrix} v \\ \beta \end{Bmatrix} = \begin{bmatrix} W^T W & W^T Q \\ Q^T W & Q^T Q \end{bmatrix}^{-1} \begin{bmatrix} W^T \\ Q^T \end{bmatrix} \{P\} \tag{19}$$

Complications may arise in practice such as a lack of information available to fully determine all system parameters. It is often preferable to solve equation (18) using the Singular Value Decomposition (SVD) method [11], although this was not necessary for the example considered in this paper. It is also found that these matrices are often complex, in which case they must be divided into their real and complex parts. These matters, the conditioning of the regression matrix and the method employed in the case where some extra knowledge of the system may be available, either from further modelling or testing, are discussed in detail in [8]. If damping is included in the model of the bearings then $[W]$, $[Q]$ and $\{P\}$ will become complex, although the system parameters it is intended to identify remain real. For the two direction case and ignoring damping effects, for two orthogonal directions z and y

$$\{v\} = \{k_{1yy} \quad k_{1zz} \quad k_{22yy} \quad k_{22zz} \quad k_{1yz} \quad k_{12yz} \quad k_{22yz} \quad k_{12yy} \quad k_{12zz} \quad k_{12yz}\}^T$$

with corresponding mass terms. The terms in $w(\omega)$ are given by $[w(\omega)] = [[\hat{w}] \quad -\omega^2[\hat{w}]]$, where

$$[\hat{w}] = \begin{bmatrix} y_{p1} & 0 & 0 & 0 & z_{p1} & 0 & 0 & y_{p2} & 0 & z_{p2} \\ 0 & z_{p1} & 0 & 0 & y_{p1} & y_{p2} & 0 & 0 & z_{p2} & 0 \\ 0 & 0 & y_{p2} & 0 & 0 & z_{p1} & z_{p2} & y_{p1} & 0 & 0 \\ 0 & 0 & 0 & z_{p2} & 0 & 0 & y_{p2} & 0 & z_{p1} & y_{p1} \end{bmatrix} \tag{20}$$

The modal coefficient vector now has components in both the z and y directions and is given by $\{\beta\} = \{\beta_{1y} \quad \beta_{1z} \quad \beta_{2y} \quad \beta_{2z}\}^T$, the resulting equation being solved in the same way as before.

3.1 INCLUSION OF UNBALANCE

The development of the identification method to include both a bend and unbalance is simply an extension of the above theory. The unbalance definition previously developed [8], where the unbalance forcing acts at a pre-determined set of d unbalance planes, at the locations $x_{e1},\ldots,x_{ed}$ is used. For a finite frequency range the unbalance may be assumed to be a summation over the balance planes, which allows equation (5) to be re-written to include unbalance forcing as

$$y_r(x) = \sum_{i=1}^{d} G(\omega, x, x_{ei})\omega^2 e_i + \sum_{m=1}^{\infty} [G_{bend}]_{mm} \hat{k}_m \beta_m \psi_m(x) + \sum_{i=1}^{n} G(\omega, x, x_{bi}) F_{bi} \tag{21}$$

where e_i is the unbalance (mass times radius) acting at each location x_{ei} Equation (13) can then be expanded, including unbalance, to

$$\{F\} = [p]\{y_p\} - [q]\{\beta\} - [u]\{e\} \tag{22}$$

where $[u] = \omega^2[a]^{-1}[k_B][G_{be}]$, $\{e\} = \{e_1, \ldots, e_d\}^T$, the unknown unbalance vector, and $[G_{be}]$ is the relationship between the bearings and the unbalance planes. For a complete treatment of the unbalance identification theory the reader is referred to [8]. Equation (22) now contains three forcing terms, in contrast to the two terms of equation (13), which, by the previous method, gives the result

$$\begin{Bmatrix} v \\ \beta \\ e \end{Bmatrix} = \begin{bmatrix} W^T W & W^T Q & W^T U \\ Q^T W & Q^T Q & Q^T U \\ U^T W & U^T Q & U^T U \end{bmatrix}^{-1} \begin{bmatrix} W^T \\ Q^T \\ U^T \end{bmatrix} \{P\} \tag{23}$$

4. NUMERICAL EXAMPLE

A rotor of length 4 m and diameter 0.2 m mounted on two bearings of stiffness 100 MN/m, supported by pedestals having stiffness 150 MN/m and mass 100 and 150 kg respectively was used for the analysis. A schematic diagram of the system is shown in Figure 1. Although it is unrealistic to hold the bearing stiffnesses constant over the speed range, this was done for the sake of clarity, in order to highlight the features of the method itself. The system has the following natural frequencies:

rotor (free-free): 56 and 154 Hz

rotor-bearing-foundation system: 23 and 72 Hz

foundations: 159 (foundation 2) and 195 Hz (foundation 1)

A series of numerical tests were performed to examine the behaviour of the method under various changes in system conditions: frequency range, step size, noise and bearing error, as shown in Table 1. The bearing error was incorporated into the analysis in 10, 20 and 50% steps and noise is introduced as a factor of either 2 or 4 times the high frequency response. In the cases using simulated noisy data, each test was performed twenty times and a mean value taken. A reference frequency range of 0-200 Hz was chosen with a step size of 1 Hz. Responses for cases 6 and 15 are shown in Figures 2 and 3, for the individual bend, with $\beta_2 = 0$, and the combined system respectively.

Tests are considered with both bend and unbalance, individually and combined. For a bend with a half-sine wave profile having maximum displacement of 0.01 m at the mid-point along the shaft central axis, the first two modal coefficients are $\beta_1 = 0.0162$ and $\beta_2 = 0$. Tests are also included for $\beta_2 = 0.01$, representing the case where the bent shaft profile is unsymmetrical. Unbalances of 1 and 2 kg.m, acting at planes at distances of 1 and 3 m respectively along the rotor, were defined.

4.1 RESULTS

In cases 1, 2, 3 and 4, where the frequency range and step size are reduced from the reference values to 100 Hz and step size = 2 Hz, with no noise or errors present, all parameters are identified correctly in each case considered for each different system. In cases 5 and 6, noise is introduced whilst performing calculations over the reference frequency range and step size: highly accurate results are shown for the identification of both foundation and bend/unbalance parameters. The maximum error is a 10% error in bend estimation.

Cases 7 and 8 demonstrate the effect of noise on a reduced frequency range of 150 Hz, with a step size of 1 Hz. *Bend*: for $\beta_2 = 0$, only with 4% noise do the results show any significant discrepancy, and then only for the foundation parameters, where there is a maximum error of 3% in foundation stiffness. For $\beta_2 = 0.01$ it is not the foundation parameters which are affected by noise but the bend coefficients, with a maximum error of 3% when the data has a noise factor of 2. *Unbalance*: the results show that both the foundation parameters and the unbalance were identified correctly in both cases. *Combined bend and unbalance*: the foundation identification remains very accurate in both cases, the maximum error in foundation parameters being 1%. A maximum error of 21% in bend estimation and 12% in unbalance estimation was found, which was considered acceptable.

Cases 9 and 10 show the effect of further reducing both frequency range and step size in the presence of noise. Both the bend and the unbalance remain well identified in the individual cases, with a maximum error of 5% in the estimation of the bend coefficients. The foundation parameters are also accurately predicted, except in the case where $\beta_2 = 0$, with the mass and stiffness identification exhibiting large variations. In the combined case, however, both foundation parameters and bend/unbalance properties remain within 2% of their correct values. It may be drawn from these tests that it is important to select an appropriate frequency range and step size, in order for all foundation parameters and bend/unbalance properties to be identified as accurately as possible.

Cases 11, 12 and 13 demonstrate the effect of 10, 20 and 50% errors in bearing stiffnesses over the reference speed range and step size. *Bend:* for $\beta_2 = 0$ the bend coefficients remain accurate until a bearing error of 50% is introduced, the error in the bend estimation being 30%. The foundation identification, however, is found to be rather sensitive in all three cases. For $\beta_2 = 0.01$ both the foundations and the bend identification suffer from this error, although the foundation parameters are more accurate than in the $\beta = 0$ case. *Unbalance:* foundation parameters are comparable to those in the case of the bend. The unbalance identification is considered acceptable until the bearing error is 50%. *Combined bend and unbalance:* both the bend and the unbalance estimation are shown to be rather sensitive to bearing error, although only with 50% bearing error do the results become nonsensical; a similar pattern is observed for the foundation identification.

Cases 14, 15 and 16 are as cases 11, 12 and 13, but with added noise as well as bearing error. It is noted that the bearing error is by far the most influential factor of the two, as the results for the previous three cases, with zero noise, remain virtually unchanged.

5. DISCUSSION

The above results illustrate, for a comprehensive range of conditions, the main features of the identification method. The selection of a suitable speed range and frequency step size, through which vibration measurements should be taken, is shown to be an important factor in achieving the most accurate results. The proposed method is then able to deal with noisy data with a high degree of precision.

Bearing error is dealt with adequately, in terms of the bend identification itself, until very large errors in the bearing stiffness terms are introduced. Foundation parameters, however, suffer to a greater degree. In the case where an acceptably accurate value of bearing stiffness is unavailable, this may be overcome by the inclusion of measurement of absolute shaft displacement at the bearings, in which case no bearing model is required [8].

Damping has been omitted from the above investigations in order to keep the analysis as clear as possible. Its incorporation is not seen as posing any serious difficulty,

although for the investigation of phase relationships, further work beyond the scope of this paper is required.

In summary, so long as suitable speed ranges are chosen, with either a fairly accurate model of the bearing or shaft displacement measurements, both the foundation parameters and bend and/or unbalance characteristics may be identified with a high degree of accuracy, even in the presence of noise.

6. SUMMARY AND CONCLUSIONS

One problem experienced in the area of rotor dynamics is the detection of shafts with a bend. It has often been the case that a bowed shaft has been confused with an unbalanced shaft, and large vibration responses remain after balancing has been performed. In this paper, a method has been shown which, given certain conditions, can accurately estimate the bend geometry and foundation mass and stiffness parameters, for a rotor-bearing system mounted on flexible supports. The identification of a bend and unbalance acting concurrently has also been successfully included in this method, which has shown itself to be suitably robust to noise and uncertainty of bearing behaviour.

7. ACKNOWLEGEMENTS

The authors are pleased to acknowledge the support of Magnox Electric Ltd. Dr. Friswell gratefully acknowledges the support of the EPSRC through the award of an Advanced Fellowship.

8. REFERENCES

[1] Nicholas, J.C., Gunter, E.J., and Allaire, P.E., *Effect of Residual Shaft Bow on Unbalance Response and Balancing of a Single Mass Flexible Rotor Part 1 - Unbalance Response,* Journal of Engineering for Power, pp. 171-181, 1976.

[2] Nicholas, J.C., Gunter, E.J., and Allaire, P.E., *Effect of Residual Shaft Bow on Unbalance Response and Balancing of a Single Mass Flexible Rotor Part 2 - Balancing,* Journal of Engineering for Power, pp. 182-189, 1976.

[3] Parkinson, A.G., Darlow, M.S., and Smalley, A.J., *Balancing Flexible Rotating Shafts with an Initial Bend,* AIAA Journal, 22, No.5, pp. 683-689, 1984.

[4] Meacham, W.L., Talbert, P.B., Nelson, H.D., and Cooperrider, N.K., *Complex Modal Balancing of Flexible Rotors Including Residual Bow,* Journal of Propulsion and Power, 4(3), pp. 245-251, 1988.

[5] Flack, R.D., Rooke, J.H., Bielk, J.R., and Gunter, E.J., *Comparison of the Unbalance Responses of Jeffcott Rotors with Shaft Bow and Shaft Runout,* Transactions of the ASME, 104, pp. 318-328, 1982.

[6] Salamone, D., and Gunter, E.J., *Synchronous Unbalance of a Multimass Flexible Rotor Considering Shaft Warp and Disk Skew,* M.Sc. Thesis No. UVA/464761/ME77/142, University of Virginia, Charlottesville, Virginia, 1977.

[7] Salamone, D.J., and Gunter, E.J., *Synchronous Unbalance Response of an Overhung Rotor with Disk Skew,* Journal of Engineering for Power, 102, pp. 749-755, 1980.

[8] Lees, A.W., and Friswell, M.I., *The Evaluation of Rotor Unbalance in Flexibly Mounted Machines,* Journal of Sound and Vibration, in press, 1997.

[9] Lees, A.W., and Friswell, M.I., *Estimation of Forces Exerted on Machine Foundations,* International Conference on Identification in Engineering Systems, Swansea, UK, pp. 793-803, 1996.

[10] Friswell, M.I., Lees, A.W., and Smart, M.G., *Model Updating Techniques Applied to Turbo-Generators Mounted on Flexible Foundations,* NAFEMS Conference on Structural Dynamics Modelling: Test Analysis and Correlation, Cumbria, UK, 1996, pp. 461-472, 1996.

[11] Golub, G., and Van Loan, C., *Matrix Computations,* John Hopkins University Press, London, 1989.

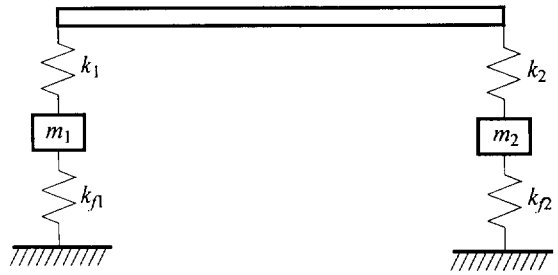

Figure 1: Flexibly supported rotor-bearing system

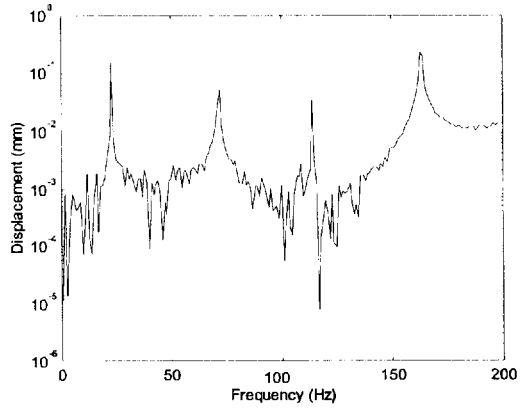

Figure 2: Combined response at bearing 1, case 6

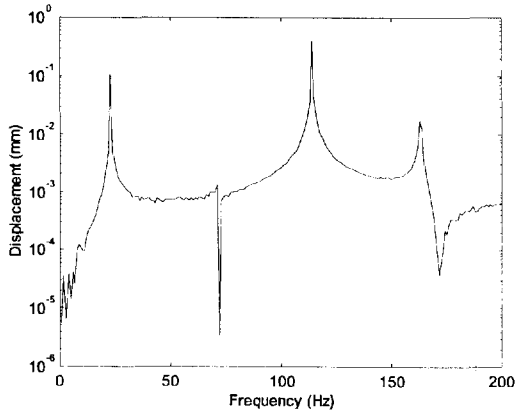

Figure 3: Bend response at bearing 2, $\beta_2 = 0$, case 15

Case	Frequency range	No. of steps	Noise	Bearing error
1	200	200	0	0
2	200	100	0	0
3	100	100	0	0
4	100	50	0	0
5	200	200	0.02	0
6	200	200	0.04	0
7	150	150	0.02	0
8	150	150	0.04	0
9	100	100	0.04	0
10	150	50	0.04	0
11	200	200	0	0.1
12	200	200	0	0.2
13	200	200	0	0.5
14	200	200	0.02	0.1
15	200	200	0.04	0.2
16	200	200	0.04	0.5

Table 1: Test cases considered

Case	K_{11} (MN/m)	K_{22} (MN/m)	K_{12} (MN/m)	M_{11} (kg)	M_{22} (kg)	M_{12} (kg)	β_1 ($\times 10^{-2}$)	β_2 ($\times 10^{-2}$)
1	150	150	0	100	150	0	1.62	0.00
2	150	150	0	100	150	0	1.62	0.00
3	150	150	0	100	150	0	1.62	0.00
4	150	150	0	100	150	0	1.62	0.00
5	150	150	0	100	150	0	1.63	0.00
6	150	150	0	100	149	0	1.62	0.00
7	150	150	0	100	150	0	1.62	0.00
8	146	146	4	98	147	2	1.62	0.00
9	119	119	31	55	101	47	1.62	-0.01
10	106	106	44	-12	40	110	1.62	0.00
11	188	188	-57	123	191	-57	1.58	0.00
12	277	277	-158	187	290	-155	1.59	0.00
13	-713	-710	812	-561	-811	764	1.14	0.01
14	188	187	-56	123	191	-57	1.58	0.00
15	274	274	-154	184	286	-152	1.59	0.00
16	-699	-696	797	-550	-795	749	1.14	0.00

Table 2: Bend identification results, $\beta_1 = 0.0162$, $\beta_2 = 0$

Case	K_{11} (MN/m)	K_{22} (MN/m)	K_{12} (MN/m)	M_{11} (kg)	M_{22} (kg)	M_{12} (kg)	β_1 ($\times 10^{-2}$)	β_2 ($\times 10^{-2}$)
1	150	150	0	100	150	0	1.62	1.00
2	150	150	0	100	150	0	1.62	1.00
3	150	150	0	100	150	0	1.62	1.00
4	150	150	0	100	150	0	1.62	1.00
5	150	150	0	100	150	0	1.62	1.00
6	150	150	0	100	150	0	1.63	1.00
7	150	150	0	100	150	0	1.57	1.00
8	150	150	0	100	150	0	1.6	0.98
9	150	150	0	100	150	0	1.62	1.00
10	140	145	-8	79	142	-17	1.54	0.99
11	126	142	-1	64	150	-3	1.36	0.91
12	102	148	-2	21	172	-4	0.9	0.85
13	201	-57	-13	302	-239	-47	3.77	0.73
14	126	142	-1	64	150	-3	1.36	0.91
15	102	148	-2	21	172	-4	0.91	0.85
16	201	-57	-13	302	-239	-47	3.77	0.73

Table 3: Bend identification results, $\beta_1 = 0.0162$, $\beta_2 = 0.01$

Case	K_{11} (MN/m)	K_{22} (MN/m)	K_{12} (MN/m)	M_{11} (kg)	M_{22} (kg)	M_{12} (kg)	e_1	e_2
1	150	150	0	100	150	0	1.00	2.00
2	150	150	0	100	150	0	1.00	2.00
3	150	150	0	100	150	0	1.00	2.00
4	150	150	0	100	150	0	1.00	2.00
5	149	149	0	99	149	-1	1.03	2.02
6	150	150	1	101	151	1	0.96	2.00
7	150	150	0	100	150	0	1.00	2.00
8	150	150	0	100	150	0	1.00	2.00
9	149	149	1	99	149	6	1.01	2.01
10	150	150	1	102	152	6	0.99	1.99
11	131	150	2	74	162	5	1.07	1.98
12	110	164	3	38	198	10	1.23	2.05
13	219	-80	28	338	-242	15	-0.11	0.62
14	131	150	3	74	162	5	1.07	1.97
15	110	164	4	37	199	10	1.22	2.05
16	214	-79	25	328	-244	9	-0.05	0.69

Table 4: Unbalance identification results

Case	K_{11}	K_{22}	K_{12} (MN/m)	M_{11} (kg)	M_{22} (kg)	M_{12} (kg)	β_1 ($\times 10^{-2}$)	β_2 ($\times 10^{-2}$)	e_1	e_2
1	150	150	0	100	150	0	1.62	0.00	1.00	2.00
2	150	150	0	100	150	0	1.62	0.00	1.00	2.00
3	150	150	0	100	150	0	1.62	0.00	1.00	2.00
4	150	150	0	100	150	0	1.62	0.00	1.00	2.00
5	150	150	0	100	150	0	1.62	-0.10	0.95	2.04
6	150	150	0	101	151	1	1.65	0.10	1.03	1.94
7	150	150	0	99	151	1	1.62	0.00	1.00	2.00
8	150	150	0	101	151	-2	1.63	0.21	1.12	1.86
9	150	150	1	102	152	8	1.60	-0.09	0.98	2.10
10	148	150	-1	93	151	-2	1.59	0.07	1.05	1.95
11	133	134	-1	79	150	5	1.37	0.41	1.28	1.66
12	120	124	-1	52	166	12	1.15	1.50	2.06	1.01
13	115	96	-4	266	-69	-1	1.44	-10.58	-6.92	7.51
14	133	134	-1	79	150	5	1.36	0.44	1.29	1.64
15	121	124	0	53	165	11	1.13	1.49	2.07	1.01
16	114	96	-4	270	-67	2	1.44	-10.73	-7.02	7.57

Table 5: Combined bend and unbalance identification results, $\beta_1 = 0.0162$, $\beta_2 = 0$